

**Crustal Seismic Anisotropy in the Martian Lowlands.** C. Beghein<sup>1</sup>, J. Li<sup>1</sup>, E. Weidner<sup>1</sup>, R. Maguire<sup>2</sup>, J. Wookey<sup>3</sup>, V. Lekić<sup>4</sup>, P. Lognonné<sup>5</sup>, and W.B. Banerdt<sup>6</sup>, <sup>1</sup>Earth, Planetary, and Space Sciences department, University of California Los Angeles, Los Angeles, CA, USA (cbeghein@epss.ucla.edu), <sup>2</sup>Department of Geology, University of Illinois Urbana-champaign, Urbana, IL, USA, <sup>3</sup>School of Earth Sciences, University of Bristol, Bristol, UK, <sup>4</sup>Department of Geology, University of Maryland, College Park, MD, USA, <sup>5</sup>Institut de Physique du Globe de Paris, Université Paris Cité, Paris, France, <sup>6</sup>Jet Propulsion Laboratory, California Institute of Technology, Pasadena, CA, USA.

**Introduction:** The seismic data collected by the InSight mission have provided unprecedented constraints on the interior structure of Mars, including the thickness of the crust, mantle structure, and the size of the core [1-6]. It also enabled the detection of seismic anisotropy, i.e. the directional dependence of seismic wave velocity, beneath the lander within the topmost crustal layer [7]. Seismic anisotropy is commonly studied on Earth and is a powerful tool to study deformation processes within a planet. The signal observed in [7] was constrained by body waves and was shown to be compatible with the presence of local East-West oriented fractures or radial dikes caused by impact cratering.

The largest seismic event ever detected on Mars, S1222a, with a moment magnitude of  $4.7 \pm 0.2$ , occurred on 4 May 2022 almost 2,200 km away from the seismometer [8]. It was the only event to produce both Love and Rayleigh wave signals. Since Rayleigh and Love waves are predominantly sensitive to different elastic parameters (governing the speed of vertically and horizontally polarized shear waves that travel horizontally, respectively), this gave us an opportunity to study the presence of seismic anisotropy over larger scales, away from the landing site [9]. Here, we present our analysis of those data and demonstrate that seismic anisotropy compatible with a vertically transverse isotropic medium is present in the crust between the seismometer and the event epicenter.

**Data Analysis:** By filtering the seismograms at different frequencies, we found that S1222a generated surface wave-like energy at periods between about 10 and 40 s on all components of the seismogram. We then conducted an ellipticity analysis of the data in multiple period bands, which showed a clear elliptical and retrograde motion between periods of 15 and 35 s, confirming the Rayleigh wave nature of the observations at these periods. We carried out a multiple filter analysis [10] of the three seismogram components to determine the group velocities as a function of time (Fig. 1). We verified that the back azimuth uncertainties did not affect the resulting dispersion curves. However, we found discrepancies in the Rayleigh wave measurements between the vertical (Fig. 1(a)) and radial (Fig. 1(b)) components at period

greater than 30 s, and thus decided to only use data between 15 and 30 s.

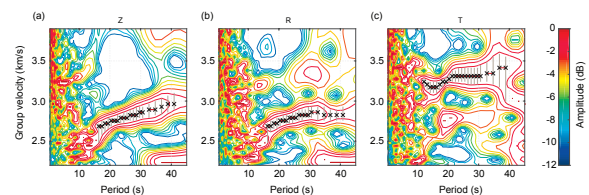


**Fig. 1:** Multiple filter analysis of the vertical (a), radial (b), and tangential (c) components of the seismogram.

**Modeling:** The measured Love and Rayleigh wave dispersion curves were inverted to obtain velocity models representing the average structure between the station and the quake. Love and Rayleigh waves provide constraints on the speed of horizontally ( $V_{SH}$ ) and vertically ( $V_{SV}$ ) polarized shear-waves, respectively. Radial seismic anisotropy can be quantified by parameter  $\xi = V_{SH}^2/V_{SV}^2$ , and the Voigt average velocity is given by  $V_S = \sqrt{(2V_{SV}^2 + V_{SH}^2)/3}$ .

We first inverted the Rayleigh wave dispersion and used the resulting models to predict Love wave dispersion, and vice versa. We were unable to explain one type of data with the models obtained by inversion of the other data type. This so-called Love-Rayleigh discrepancy has been widely observed on Earth and can be resolved by introducing radial anisotropy, also called vertical transverse isotropy, in the model [11]. The period range considered corresponds to sensitivity to anisotropy in the upper  $\sim 80$  km and to isotropic velocities down to  $\sim 130$  km.

We tested three different inversion methods, hereafter referred to as Method 1, 2, and 3, based on different model-space search approaches and different forward modeling codes. We also tested whether isotropic models could explain the data equivalently well by imposing  $V_{SV} = V_{SH}$  in our inversions.

**Results and Interpretation:** The isotropic inversions resulted in models that did not fit the data as well as the anisotropic models, and statistical F-tests showed that the improvement in data fit when anisotropy is introduced is significant. We thus proceed with the analysis of our anisotropic inversions.

The posterior Voigt average  $V_s$  model distribution displays large uncertainties (Fig. 2) and varies significantly between methods in the top 5 km and below 30 km depth [9]. Between 5 and 10 km depth, Methods 1 and 2 predict  $V_s = 3.0 \pm 0.1$  km/s and  $V_s = 3.2 \pm 0.1$  km/s, respectively, and Method 3 gives  $V_s$  between  $2.5 \pm 0.3$  km/s and  $3.0 \pm 0.75$  km/s. These values are compatible with damaged or altered basalt, but also with impact melt, impact breccia, and sandstone [12]. Between  $\sim 10$  and 30 km depth,  $V_s$  is consistent among the three methods with values around 3.1–3.5 km/s, compatible with volcanic rocks (damaged, altered, or compact basalt) and with impact melt.

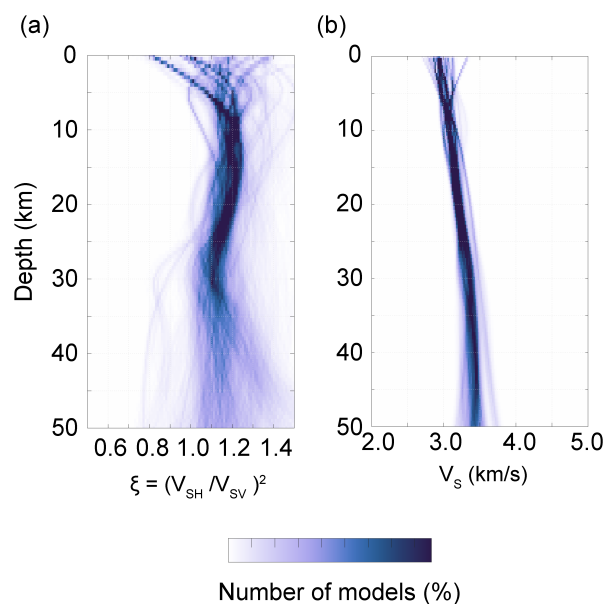


**Fig. 2:** Anisotropy (a) and velocity (b) models resulting from inverse Method 1 applied to the measured dispersion curves.

Our results also indicate a robust seismic anisotropy signal with  $V_{SH} > V_{SV}$  in the 10 – 30 km depth range (Fig. 2), which corresponds to crustal depths [3, 13]. Lattice Preferred Orientation of intrinsically anisotropic crystals in the Martian crust is unlikely to explain these observations as it would require strain coherent over large scales, such as underthrusting or large-scale crustal thinning, and we do not have any evidence for it on Mars. We also rule out the alignment of cracks as the origin of this signal since cracks tend to close at those pressures [14].

Horizontal layering of isotropic material with layer thicknesses much smaller than the dominant wavelength is a more likely explanation [15]. While such a mechanism could result from sediment deposits over large distances, we rule it out because the

estimated global average thickness of the sediment layer is less than 2 km [16]. Alternatively, the presence of layered intrusions due to a single or multiple impacts [17] or an alternation of basalt layers deposit and sedimentation due to multiple volcanic events over broad scales might generate an anisotropy signal similar to what we observe.

We note that, owing to the different depth ranges and the local vs regional aspect of the two studies, the anisotropy revealed here by the surface waves, i.e., a transversely isotropic medium with vertical symmetry axis, does not contradict the signal found with body waves beneath the lander [7], which itself can be reproduced by a horizontally transversely isotropic medium.

**Acknowledgments:** We acknowledge NASA, CNES, their partner agencies and institutions (UKSA, SSO, DLR, JPL, IPGP-CNRS, ETHZ, IC and MPS-MPG) and the flight operations team at JPL, SISMOC, MSDS IRIS-DMC and PDS for delivery of SEIS data and operating the InSight mission. The InSight seismic waveforms are available at the IPGP Datacenter, NASA-PDS and IRIS-DMC [18,19]. This research was carried out in part at the Jet Propulsion Laboratory, California Institute of Technology, under a contract with the National Aeronautics and Space Administration (80NM0018D0004). C. B., J. L., and E.W. were funded by NASA InSight PSP Grant 80NSSC18K1679. J.W. was funded by UKSA Aurora Grant ST/T002972/1. PL is funded by the french space agency, CNES and by Agence Nationale de la recherche (ANR-19-CE31-0008-08 and ANR-18-IDEX-0001).

**References:** [1] Khan et al. (2021), *Science*, 373, 434–438. [2] Knapmeyer-Endrun, B. et al. (2021), *Science*, 373, 438–443. [3] Stähler, S. C. et al. (2021), *Science*, 373, 443–448. [4] Huang et al (2022), *PNAS*, 119. [5] Kim et al. (2022), *Science*, 378, 417–421. [6] Li, J. et al. (2022), *Nat. Commun.*, 13, 7950. [7] Li et al. (2022), *epsl*, 593, 117654. [8] Kawamura et al. (2022), *GRL*, 49, e2022GL101543. [9] Beghein et al. (2022), *GRL*, 49, e2022GL101508. [10] Hermann (2013), *SRL*, 84(6), 1081–1088. [11] Anderson (1961), *JGR*, 66(9), 2953–2963. [12] Lognonné et al. (2020), *Nat Geo*, 13, 213–220. [13] Wiecezorek et al. (2022), *JGR: Planets*, 127, e2022JE007298. [14] Crampin (1981), *Wave Motion*, 3(4), 343–391. [15] Backus (1962), *JGR*, 67(11), 4427–4440. [16] McLennan (2012), in *Sedimentary geology on Mars*. [17] Andrews-Hanna et al. (2008), *Nat*, 453(7199), 1212–1215. [18] InSight Mars SEIS Data Service (2019), 10.18715/SEIS/INSIGHT.XB.2016. [19] InSight SEIS Science Team (2019), 10.17189/1517570.